

INVESTIGATING THE TRANSFER OF HEAT BETWEEN  
A VIBRATION-FLUIDIZED BED OF DISPERSE  
MATERIAL AND A BODY THAT IS BEING  
COOLED WITHIN THIS MATERIAL

I. I. Kal'tman and A. I. Tamarin

UDC 541.182.3

We investigate the intensity of heat transfer between spherical  $\alpha$  calorimeters and a vibration-fluidized bed. The experimental data are generalized in the form of criterial relationships.

Certain technological processes in the metallurgical and machine-building industry [1-3] are best accomplished in a fluidized bed. In a number of cases, e.g., in the hardening of component parts, the use of a vibration method of fluidization offers a number of distinct advantages [4, 5]. To develop industrial installation involving the use of a vibration-fluidized bed, we must know the fundamental quantitative relationships governing the transfer of heat between this medium and the material immersed in it. The literature has given inadequate attention to this problem. There are a few data for a narrow range of variations in the vibration parameters, derived for a low temperature of the heat-exchange surface (below 300°C) [6-13, 26]. It is the purpose of this investigation to determine some of the quantitative relationships governing the transfer of heat in cooling of hot objects (850°C) in a vibration-fluidized bed.

A cylindrical vessel 140 mm in diameter and 300 mm in height was attached to the platform of the vibrator, and the walls of the vessel were cooled with water. The tests were carried out with a variety of disperse materials, whose characteristics are given in Table 1.

The material was poured into the vessel to a height of 70-80 mm in each of the experiments; electro-mechanical vibrators were used in the tests: a cam-driven vibrator and one based on the time-delay (unbalance) principle. The platforms of the two vibrators, for all intents and purposes, executed vertical oscillations. The frequency control for the cam-driven vibrator was achieved by changing the drive pulleys, and the amplitudes were regulated by altering the eccentricity. The parameters of the time-delay vibrator were regulated by turning the unbalances and altering the supply voltage for the dc electric motor. A tachometer accurate to 3% was used to measure the vibration frequency. The vibrator stands were designed so as to produce the following maximum vibration parameters; amplitudes of 8 and 12 mm for frequencies of 19 and 16.8 Hz, respectively, on the cam-driven vibrator, and amplitudes of 6.4 and 3 mm at frequencies of 16.8, 32, and 36 Hz respectively, for the time-delay vibrator.

During the experiments we measured the heat-transfer coefficient by means of a heat probe (an  $\alpha$  calorimeter), which was made of a copper or a nickel sphere into whose center a Chromel-Alumel thermocouple had been imbedded. The heat probe, first heated in an electric furnace to a temperature of 850-900°C, is rapidly immersed into the vibrating bed along the axis of the vessel and it is fixed at the midpoint of the charge height. The temperature of the vibrating bed during the experiment did not go above 40°C. During the cooling of the heat probe, an automatic potentiometer recorder (class 0.5, time of scale coverage 1 sec) to mark the temperature difference between the bed and the probe ( $\theta$ ), measured by the differential thermocouple. The heat-transfer coefficient is determined by a regular-regime method on the basis of the heat-probe cooling rate [16] in the vibration-fluidized bed, i.e.,

$$\alpha = \frac{m_h V_h c_h \theta_h}{S_h \Psi}$$

---

Institute of Heat and Mass Transfer, Academy of Sciences of the Belorussian SSR, Minsk. Translated from *Inzhenerno-Fizicheskii Zhurnal*, Vol. 16, No. 4, pp. 630-638, April, 1969. Original article submitted June 12, 1968.

© 1972 Consultants Bureau, a division of Plenum Publishing Corporation, 227 West 17th Street, New York, N. Y. 10011. All rights reserved. This article cannot be reproduced for any purpose whatsoever without permission of the publisher. A copy of this article is available from the publisher for \$15.00.

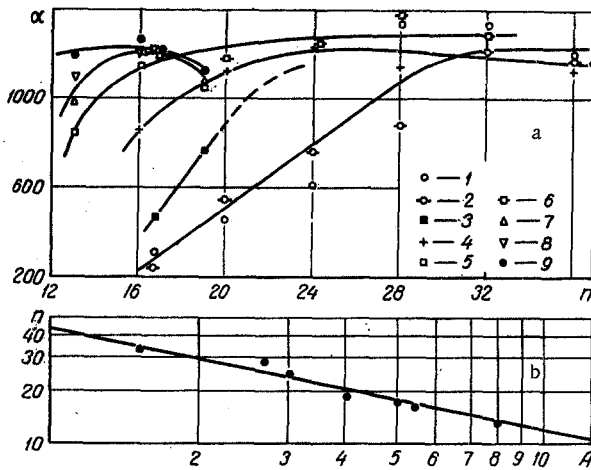


Fig. 1. Effect of vibration parameters on the intensity of heat transfer for corundum when  $d_{av} = 45.9 \mu\text{m}$ : a)  $\alpha$  ( $\text{W}/\text{m}^2 \cdot \text{deg}$ ) as a function of the frequency  $n$  (Hz) of vessel vibration; 1, 3, 5, 7, and 9) cam-driven vibrator; 2, 4, 6, and 8) time-delay vibrator; 1 and 2)  $A = 1.5$  mm; 3) 2 mm; 4) 3 mm; 5 and 6) 4 mm; 7 and 8) 6 mm; 9)  $A = 8$  mm; b) interrelationship between optimum vibration parameters: frequencies  $n$  (Hz) and amplitudes  $A$  (mm).

where  $m = \ln \theta_1 / \theta_2$ ,  $1/\tau$  is the cooling rate, and  $\Psi$  is a coefficient by means of which we take into consideration the magnitude of the temperature gradient through the cross section of the  $\alpha$  calorimeter.

As they were being processed, the  $\theta(\tau)$  curves in the range from 850 to 100°C were divided into segments of 50°C, within whose limit the magnitude of  $\alpha$  could be regarded as virtually constant. The resulting value of  $\alpha$  was referred to the average surface temperature for each theoretical segment. Such a procedure made it possible graphically to plot the function  $\alpha(\theta)$  for the entire cooling period. From three to five thermograms of  $\theta(\tau)$  were taken for each material in a given vibration regime.

To increase experimental accuracy, the graph paper of the electronic potentiometer was made to move at a speed such that the maximum time-measurement error did not exceed 3-4%.

The measurement accuracy is primarily affected by the error in the determination of the cooling rate that is dependent on the absolute error in the recording of the temperatures.

To reduce the absolute error in the temperature measurement, the potentiometer was graduated from 17 to 37 mV. To record temperatures up to 480°C, an additional emf was introduced into the measuring circuit from a stable-voltage source. The maximum relative error in the determination of the heat-transfer coefficient was thus no more than  $\pm 14\%$ .

One of the basic factors governing the intensity of heat transfer in the medium under consideration is the hydrodynamic regime of that medium. The kinetic energy transmitted to the bed by the vibration of the vessel is transformed into the kinetic energy of the moving particles. Similar to the fluidized bed, stable low-frequency large-scale circulation loops for groups of particles are seen in the system, and simultaneously we find high-frequency small-scale loops. A statistical steady-stage [25] field of particle velocities and their groups is set up in the bed. This field can be described, to a first approximation, by the mean square mass velocity  $\bar{u}$  and the average scale (dimension)  $\bar{l}$  of the circulation loops. Proceeding from these concepts, within brief time intervals continuous replacement of the particle groups takes place at the surface immersed in the bed. The average contact time for the particle group is proportional to the circulation time

$$\tau_{\text{eff}} = \frac{1}{f_{\text{eff}}} = \frac{\bar{l}}{u}.$$

This relationship will be valid if the surface dimension is greater than the average dimension of the particle circulation loop within the bed. In this case, the time of contact between the particle group and the wall will be independent of the geometric dimensions of the immersed body.

The transfer of heat from the surface to the vibration-fluidized bed can thus be treated as a process of heating continuously changing groups of particles. The removal of heat by the gas leaving the bed, because of its low heat capacity, is negligibly small. The radiative heat exchange, according to our estimates, is also slight and it can be neglected. Convection (filtration) heat transfer for small Re numbers (rather small particles), when the streamlining is primarily without separation, on the basis of the estimates from [17, 21], was also not considered. The particle group together with the gas that it contains, as a first approximation, will be treated as a packet in which the transfer of heat is achieved as a consequence of an effective

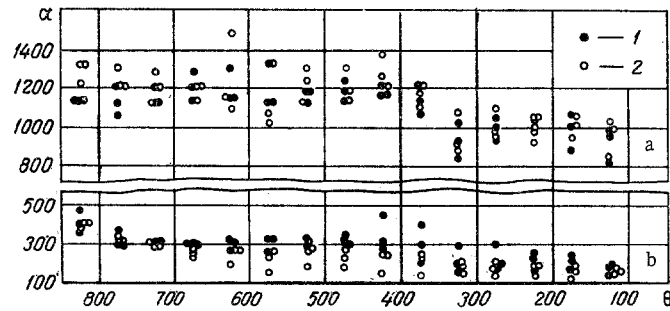


Fig. 2. Heat-transfer coefficient  $\alpha$  ( $\text{W}/\text{m}^2 \cdot \text{deg}$ ) of a vibration-fluidized bed of corundum for  $d_{av} = 45.9 \mu\text{m}$  (with a surface) as a function of the excess temperature  $\theta$  ( $^{\circ}\text{C}$ ): a)  $n = 16.8 \text{ Hz}$ ,  $A = 6 \text{ mm}$ ; b)  $n = 16.8 \text{ Hz}$ ,  $A = 1.5 \text{ mm}$ ; 1) cam-driven vibrator; 2) time-delay vibrator.

thermal conductivity  $\lambda_p$  which is a function of porosity, as well as of the thermal conductivities of the gaseous and solid phases. Assuming that the packet is heated in a manner analogous with the heating of a semi-infinite body, we find that the intensity of heat transfer from the wall to the packet can be defined [15] in the following manner:

$$q = -\sqrt{\lambda_p \rho_p c_p} \Delta t \frac{1}{\sqrt{\pi \tau}}.$$

The average heat flow during the time  $\tau$

$$\bar{q} = \frac{1}{\tau} \int_0^{\tau} q d\tau = \frac{2\sqrt{\lambda_p \rho_p c_p}}{\sqrt{\pi \tau}} \Delta t. \quad (1)$$

Analogous concepts were used earlier [18, 19, 21] for the fluidized bed.

Using the familiar notation, we can write Eq. (1) in the form of the criterial relationship

$$\text{Nu} \sqrt{\text{Fo}} = \frac{2}{\sqrt{\pi}}. \quad (2)$$

It follows from (2) that the heat-transfer intensity in the investigated medium varies in inverse proportion to the square root of the dimensionless time of contact between the packet and the wall, which is a function of the ratio  $l/u$ . To eliminate the effect of the circulation-loop dimension on heat transfer, we must make the diameter of the  $\alpha$  calorimeter greater than  $\bar{l}$ . In this connection, we performed tests with five  $\alpha$  calorimeters of various diameters in vibration fluidized corundum with an average particle dimension of  $68.4 \mu\text{m}$  for  $n = 16.8 \text{ Hz}$  and  $A = 4 \text{ mm}$ . The results of these tests are given in Table 2. The values of  $\alpha$  correspond to the range of temperatures for the probe surface from  $650$  to  $700^{\circ}\text{C}$ . The table gives the arithmetic mean values from the data of three measurements.

It follows from the table that a change in probe diameter by a factor of 2.4 has virtually no effect on the heat-transfer intensity. This obviously indicates that the probe dimensions were greater than the average scale of the circulation loop. In subsequent experiments we used a probe with a diameter of  $20 \text{ mm}$ .

The main series of tests were carried out over a wide range of frequencies and amplitudes on corundum powders with an average grain diameter of  $45.9 \mu\text{m}$ .

The results of this series of experiments are given in Fig. 1. We can see from the curve in Fig. 1a that over the entire investigated range of vibration parameters, for specific frequencies, we note bends in the curves for  $\alpha = f(n)$ . Here, the greater the amplitude, the lower the frequencies at which the curve bends. The presence of a maximum in the intensity of the transfer of heat between the surface and the vibration-fluidized bed was also noted by other researchers [6, 7, 11]. As we can see from the cited data, the coefficient of heat transfer is a nonmonotonic function of the amplitude and frequency. The extremum condition for this function is

TABLE 1. Characteristics of the Test Materials

Material	$d_{av}, \mu\text{m}$	$\rho_{\text{part}}, \text{kg/m}^3$	$\varepsilon$	Limits of vibration in vibration parameters		Particle shape
				A, mm	n, Hz	
Corundum	287,9	4000	0,537	4; 8	16	Irregular, acute-angled
"	125,8	4000	0,57	4	16,8	The same
"	102,7	4000	0,585	6,8	16	"
"	68,4	4000	0,562	2-12	13-24	"
"	45,9	4000	0,562	1,5-8	13-36	"
"	14,2	4000	0,622	4; 6	16	"
"	10	4000	0,71	4; 6	16	"
"	7	4000	0,77	4; 6	16	"
Sand	470,8	2500	0,428	6	16; 16,8	Acute-angled
"	282	2500	"	2-6	16-28	"
"	201	2500	0,43	3-6	16-36	"
"	82,4	2500	0,456	4-8	16; 16,8	"
Carborundum	79,1	3200	0,569	6-8	16	Irregular, acute-angled
Copper	26,2	8930	0,814	4; 6	16	The same
Iron	79,8	7880	0,658	4	16,8	"
Magnesite	159,9	3100	0,513	4	16,8	Acute-angled
Chamotte clay	41,8	2650	0,615	4	16,8	"
Cast iron shot	1000	7850	0,445	4; 6	16,8	Circular
Nickel	400	8900	0,57	4	24	"

$$\frac{\partial \alpha(A, n)}{\partial n} = 0 \text{ and } \frac{\partial \alpha(A, n)}{\partial A} = 0,$$

whence  $A = f_1(n)$ .

To determine the form of this function, we processed the experimental data for corundum (45.9  $\mu\text{m}$ ) in A, n coordinates for the points corresponding to  $\alpha_{\text{max}}$ . The experimental points are shown in Fig. 1b in a logarithmic coordinate system. The experimental data fall satisfactorily on the straight line described by the following function:

$$A = 0.4 n^{-1.6}.$$

This equation can be written in the form

$$A\omega^{1.6} = 7.6 \text{ or } K = 0.78 \omega^{-0.4}.$$

The resulting relationship defines the conditions for the onset of maximum intensity in the transfer of heat between the vibration-fluidized bed and the surface. Under the conditions of our experiments, the  $\alpha_{\text{max}}$  value was reached as soon as  $K = 4.7$  (greater values of K correspond to greater frequencies).

The presence of a virtually constant value for the maximum heat-transfer coefficient evidently suggests that the effective time  $\tau_{\text{eff}}$  for the contact between the particle groups (packets) and the heat-exchange surface within the investigated range of vibration parameters is a constant quantity. We can assume that the value of the average mass flow rate for the particles remains constant in this case, i.e., with  $K \geq 0.78 \cdot \omega^{0.4}$ , in addition to the increase in the linear velocity, there is a simultaneous increase in the porosity of the bed.

For a number of technological processes, in which it is important to achieve the greatest heat-transfer coefficient (for example, in the case of hardening), it is advisable to use a regime whose vibration parameters are governed by conditions (3) and (4).

Since two types of vibrators were being used in the experiments, it was a matter of some interest to compare the experimental data derived under identical conditions, but with different vibrators. These data are presented in Fig. 2 in the form of a graph for the function  $\alpha = f_2(\theta)$ . It follows from the graph that the type of vibrator had no effect on the intensity of heat transfer.

Moreover, it can be concluded that the coefficient of the transfer changes only slightly with a variation in temperature. Thus, in studying the materials listed in Table 1 we found that as the probe was cooled from 850 to 100°C the heat-transfer intensity diminished basically by no more than 20-45%.

From the standpoint of hardening, the greatest interest is the temperature range from 530 to 730°C [20] — the so-called interval of minimum austenite stability, in which the greatest cooling rate is required. In this connection, further generalization was undertaken for this temperature interval of the cooled surface, and for the experimental values of the heat-transfer coefficient we took the average for this interval.

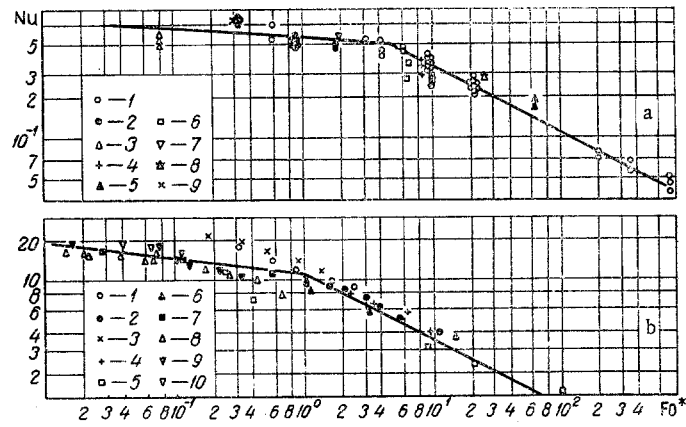


Fig. 3. Correlation of experimental data on heat transfer with respect to the surface: a) in the vibration-fluidized bed: 1) corundum; 2) sand; 3) cast iron shot; 4) corborundum; 5) copper; 6) iron; 7) magnesite; 8) chamotte clay; 9) nickel; b) in a tightly packed moving bed [22-24] ( $Nu \cdot 10$  along the axis of ordinates): 1) glass beads  $d_{av} = 375 \mu m$  in an atmosphere of air [23]; 2) the same, in a Freon atmosphere [23]; 3) glass beads  $d_{av} = 145 \mu m$  in an air atmosphere [23]; 4) the same, in a Freon atmosphere [23]; sand  $d_{av} = 150 \mu m$  in an air atmosphere [22]; 5) the same,  $d_{av} = 400 \mu m$  [22]; 7) the same,  $d_{av} = 600 \mu m$  [22]; 8) slag beads  $d_{av} = 780 \mu m$  in an air atmosphere [24]; 9) the same,  $d_{av} = \mu m$  [24]; 10) the same,  $d_{av} = 2200 \mu m$  [24].

TABLE 2. Heat-Transfer Coefficient as a Function of Heat-Probe Diameter

Diameter, mm	17,25	20	26	30	41
$W/m^2 \cdot deg$	1039	1039	940	1042	1150

We generalized all of the experimental data derived in the optimum vibration regime (i.e., when the heat-transfer intensity approaches or has actually reached the maximum value) in the form of the function  $Nu = \varphi(Fo)$ .

The coefficients of thermal conductivity and thermal diffusivity for the packet in the values of  $Nu = \alpha_{exp} d_{av} / \lambda_p$  and  $Fo = a_p \tau_{exp} / d_{av}^2$  were determined from the formulas

$$a_p = \frac{\lambda_p}{c_{part} \rho_{part} (1 - \epsilon) + c_g \rho_g \epsilon}$$

and [21]

$$\lambda_p = \lambda_r \left[ 1 + \frac{(1 - \epsilon) \left( 1 - \frac{\lambda_g}{\lambda_{part}} \right)}{\frac{\lambda_g}{\lambda_{part}} + 0.28 \epsilon^{0.63} (\lambda_{part} / \lambda_g)^{0.18}} \right]$$

In these equations the determining temperature was assumed to be equal to the mean integral temperature of the packet, which was calculated as in the case of a semi-bounded body [15] under boundary conditions of the first kind, on the basis of the formula

$$\bar{\vartheta} = \frac{1}{x} \int_0^x \text{erf}(x) dx.$$

When  $x = 1/2\sqrt{Fo} \rightarrow 2$  we have  $\bar{\vartheta} \approx 0.72$ .

As was noted, above, in an optimum vibration regime the contact time  $\tau_{eff}$  is a constant quantity. It was calculated on the basis of (1), which according to [27] is valid for large values of the Fo number:

$$\tau_{eff} = \frac{4\lambda_p c_p \rho_{part} (1 - \epsilon)}{\pi \alpha_{exp}^2} \quad (5)$$

The calculations performed for particles with an average diameter of  $d_{av} < 100 \mu\text{m}$  under the condition that the quantity  $\varepsilon$  is equal to the porosity of the bed in the free-flowing state demonstrated that the mean effective frequency  $f_{\text{exp}} = 1/\tau_{\text{eff}}$  is approximately equal to 3 Hz.

The experimental data for all of the test materials are shown in Fig. 3a. It follows from the curve that for values of  $Fo^* > 5$  the experimental data are rather well described by (2) for the system being studied. The maximum scattering in the experimental points is less than 50%. This confirms the validity of the original hypotheses with regard to the mechanism of heat transfer for the given region of  $Fo^*$  values.

For the region  $Fo^* < 5$  the quantity  $Nu$  depends only slightly on  $Fo^*$  (approximately 0.05).

For purposes of comparison, Fig. 3b shows the experimental data derived by certain authors [22-24] in measuring the coefficient of heat transfer between a moving sensor and a tightly packed bed of particles (or, conversely, for a moving bed and a fixed sensor), i.e., when the frequency of particle replacement of the surface is known. As we can see from the graph, the transfer of heat in the tightly packed bed when  $Fo > 1$  is described quite satisfactorily by the same equation (2). The maximum scattering in this case does not exceed 60%. When  $Fo < 1$ , the curves in Fig. 3a and b are virtually equidistant.

The difference between the magnitude of  $Nu$  and the values of  $Fo$  and  $Fo^*$  at the bends in the  $Nu(Fo)$  curves for tightly packed and vibration-fluidized beds is explained by the fact that the thermophysical characteristics of the packet were included in Eq. (5) for the calculation of  $\tau_{\text{eff}}$ , and the packet exhibited the porosity of a free-flowing material. Observations show that the porosity of the vibration-fluidized bed in the experiment (for  $\alpha_{\text{max}}$ ) was greater by 20-30% than that of the free-flowing material. If we convert the values of  $Nu$  and  $Fo^*$  for the vibration-fluidized bed, with consideration of the thermophysical characteristics, in the case of a porosity elevated by 20-30% (in comparison with a free-flowing material), the graphs of the  $Nu(Fo)$  functions in Fig. 3a and b virtually coincide. This indicates that the heat-transfer mechanism in a moving tightly packed and vibration-fluidized bed is identical. For small  $Fo$  numbers, when the function  $Nu(Fo)$  is weak, the basic thermal resistance is concentrated near the first row of particles and the transfer of heat is determined by the nature of the transport at the boundary between the packet and the surface.

Taking the porosity of the free-flowing material as the characteristic quantity for a vibration-fluidized bed, we can write the equations which approximate the experimental data:

for  $800 > Fo^* > 5$

$$Nu = 1.13 (Fo^*)^{-0.5}, \quad (6)$$

for  $5 > Fo^* > 0.07$

$$Nu = 0.557 (Fo^*)^{-0.064}. \quad (7)$$

These relationships may be used to calculate the maximum coefficient of heat transfer between a vibration-fluidized bed and the surface immersed within that bed. It follows from these relationships that the intensity of heat transfer is governed primarily by the thermophysical characteristics of the bed (of the material charge) and the particle dimensions. The relationship between  $\alpha$  and the particle dimensions is complex. Initially, as the Fourier number increases (a reduction in particle dimensions) the heat-transfer coefficient increases (Eq. (7)). This relationship gradually weakens, and when  $Fo \geq 5$  a change in particle dimension has no effect on the heat-transfer coefficient (Eq. (6)).

A reduction in particle diameter below approximately  $80 \mu\text{m}$  ( $Fo \geq 5$ ) is thus not advisable, since it does not result in an intensification of heat transfer.

#### NOTATION

$\alpha$	is the heat-transfer coefficient;
$a$ and $\lambda$	are the coefficients of thermal diffusivity and thermal conductivity;
$c$	is the specific heat capacity;
$A$ and $n$	are the amplitude and frequency of vessel vibration;
$\omega$	is the angular velocity;
$K = A\omega^2/g$	is the relative acceleration, where $g$ is the acceleration of free fall;
$q$	is the heat flow;
$\varepsilon$	is the porosity;

$d_{av}$	is the average particle diameter;
V and S	are the volume and area of the surface;
t	is the temperature;
$\Delta t$ and $\theta$	are the temperature differences;
$\delta$	is the relative error;
$\vartheta = (t_x, \tau - t_w)/(t_0 - t_w)$	is the relative temperature;
$t_x, \tau$	is the instantaneous temperature value;
$t_w$	is the wall temperature;
$t_0$	is the initial temperature or the temperature of the bed core;
Nu, Fo, and Re	are the similarity criteria;
Fo*	is the Fourier number in the optimum vibration regime (for a constant contact time);
$\bar{l}$	is the average dimension of the particle circulation loop;
$\bar{u}$	is the mean square mass flow rate;
$\tau_{eff}$ and $f_{eff}$	are the effective time and frequency of packet replacement.

### Subscripts

p	denotes the packet;
g	denotes the gas;
part	denotes the particle;
h	denotes the heat probe;
exp	denotes the experiment;
eff	denotes effective;
av	denotes average.

### LITERATURE CITED

1. F. S. Novik, Heat Treatment of Metals and Alloys (Survey) [in Russian], Trudy TsNIIPI, Moscow (1966).
2. M. B. Gutman, L. A. Mikhailov, and O. I. Rozhdestvenskii, Vestnik Élektropromyshlennosti, No. 8 (1963).
3. M. Tamalet, Bull. Inform. Heyrtey, No. 30 (1966).
4. A. I. Tamarin, I. I. Kal'tman, and L. A. Vasil'ev, Metallovedenie i Termicheskaya Obrabotka Metallov, No. 3 (1968).
5. I. I. Kal'tman, B. E. Sheindlin, A. I. Tamarin, L. A. Vasil'ev, and I. L. Zamnius, Trudy ONTÉI SKB-3, No. 1, Minsk (1967).
6. A. I. Tamarin, S. S. Zabrodskii, and I. L. Zamnius, in: Heat and Mass Transfer in Industrial Processes and Equipment [in Russian], Nauka i Tekhnika, Minsk (1966).
7. E. Yu. Laikovskaya and N. I. Syromyatnikov, Izvestiya Vuzov, Énergetika, No. 10 (1966).
8. T. M. Reed and M. R. Fenske, Ind. Eng. Chem., No. 2 (1955).
9. S. Brettschneider et al., Khimicheskaya Promyshlennost', No. 3 (1963).
10. V. A. Chlenov and N. V. Mikhailov, The Drying of Free-Flowing Materials in Vibration-Fluidized Beds [in Russian], Moscow (1967).
11. S. S. Zabrodskii, I. L. Zamnius, S. A. Malyukovich, and A. I. Tamarin, Inzh.-Fiz. Zhur., 14, No. 3 (1968).
12. A. S. Ginzburg and V. I. Syroedov, Inzh.-Fiz. Zhur., 9, No. 6 (1965).
13. E. Yu. Laikovskaya, B. G. Sapozhnikov, and N. I. Syromyatnikov, in: Heat and Mass Transfer Vol. 5 [in Russian], Nauka i Tekhnika, Minsk (1968).
14. I. I. Kal'tman and A. I. Tamarin, Trudy ONTÉI SKB-3, No. 1, Minsk (1967).
15. A. V. Luikov, The Theory of Heat Conduction [in Russian], Vysshaya Shkola, Moscow (1967).
16. G. M. Kondrat'ev, A Regular Heat Regime [in Russian], GTTI, Moscow (1954).
17. S. S. Zabrodskii, Hydrodynamics and Heat Transfer in a Fluidized Bed [in Russian], GÉI, Moscow - Leningrad (1963).
18. A. P. Baskakov, Inzh.-Fiz. Zhur., 6, No. 11 (1963).
19. H. S. Mickley, D. F. Fairbanks, and P. D. Hawthorn, Report No. 8 at the Fourth Conference on Heat Transfer of the A. I. Ch. E. ASME, 14-17 August 1960, New York [Russian translation].

20. A. A. Popov and L. E. Popova, "Isothermal and thermokinetic diagrams for the disintegration of supercooled austenite," Handbook for the Thermodynamicist [in Russian], Metallurgiya, Moscow (1965).
21. N. I. Gel'perin, V. G. Ainshtein, and A. V. Zaikovskii, Khimicheskaya Promyshlennost', No. 6 (1966).
22. R. Ernst, Chem. Eng. Techn., 31, No. 3 (1959).
23. N. K. Harakas and K. O. Beatty, Chem. Eng. Progr. Simpos. Series, No. 41 (1963).
24. A. I. Tamarin, V. D. Donskii, and L. V. Gorbachev, Inzh.-Fiz. Zhur., 13, No. 4 (1967).
25. A. I. Tamarin, I. Z. Mats, and G. G. Tyukhai, in: Heat and Mass Transfer, Vol. 5 [in Russian], Nauka i Tekhnika, Minsk (1968).
26. I. L. Zamnius, A. I. Tamarin, and S. S. Zabrodskii, in: Heat and Mass Transfer, Vol. 5 [in Russian], Nauka i Tekhnika, Minsk (1968).
27. N. V. Antonishin, L. E. Simchenko, and L. B. Gorbachev, in: Heat and Mass Transfer, Vol. 5 [in Russian], Nauka i Tekhnika, Minsk (1968).